THE ASTROPHYSICAL JOURNAL, 447:262–278, 1995 July 1

A SURVEY OF PLANETARY NEBULAE AT Na D: EVIDENCE FOR NEUTRAL ENVELOPES

HARRIET L. DINERSTEIN, CHRISTOPHER SNEDEN, AND JOHN UGLUM[1]
Astronomy Department and McDonald Observatory, University of Texas at Austin, Austin, TX 78712; harriet@astro.as.utexas.edu
Received 1994 August 5; accepted 1995 January 13

ABSTRACT

We present high-dispersion spectra of 21 planetary nebulae in the region of the Na I D lines at $\lambda\lambda$5889, 5895. These reasonance lines, long used to study neutral interstellar clouds, act as tracers of cool, neutral material associated with the ionized nebulae. Over half the observed objects show nebular components in the Na D lines, either in absorption or emission, or both; some of these were not previously suspected to contain neutral material. For objects in which well-resolved absorption components are seen in the Na I lines, we estimate column densities using the doublet-ratio method, finding $N(\mathrm{Na\ I}) \approx 10^{11-13}$ cm^{-2}. For five objects previously detected at 21 cm, we estimate the ratios $N(\mathrm{Na\ I})/N(\mathrm{H\ I})$. The values for the planetary nebulae are somewhat higher than for typical interstellar clouds, indicating that, integrated through the absorbing column, a larger fraction of the sodium is neutral. The layers where the Na I lines are formed generally appear to be expanding at similar velocities as the ionized gas, a result previously found for H I. A couple of objects show blue wings in the nebular Na absorptions, possibly indicating acceleration, nonspherical ejection, or the presence of clumps of low-ionization, fast-moving material.

Our results imply that the outer portions of many planetary nebulae are neutral. Therefore, the nebulae are radiation-bounded rather than mass-bounded, and the total masses are larger than the ionized masses. Resonance lines such as the Na I lines offer a means of detecting circumnebular material whether or not molecules are present, and of investigating properties of the neutral envelopes such as ionization balance, column densities, and kinematics.

Subject headings: circumstellar matter — planetary nebulae: general

1. INTRODUCTION

Evidence that many planetary nebulae possess residual neutral envelopes in addition to the more apparent ionized cores has been growing rapidly over the last few years. Most of the evidence has come from the infrared and radio spectral regions, where virtually all of the strong emission lines from cool neutral and molecular gas occur. These indicators include: the 21 cm H I line (Taylor, Gussie, & Pottasch 1990); low-J rotational transitions of CO (Huggins & Healey 1989); far-infrared lines such as [O I] 63 μm and [C II] 157 μm (Dinerstein, Haas, & Werner 1991); and the near-infrared vibration-rotation transitions of H_2 (Zuckerman & Gatley 1988; Dinerstein et al. 1988). These emission lines trace various constituents of the neutral and molecular envelopes and depend in differing ways on local physical parameters such as density, temperature, and the UV radiation field. Ongoing studies of these different probes are revealing a new picture of planetary nebulae in which the ionized zone, so prominent at optical, ultraviolet, and radio wavelengths, is only part of a larger structure that represents the cumulative recent mass loss from the progenitor star (see reviews by Rodriguez 1989; Dinerstein 1991, 1995; Huggins 1992, 1993).

The classical early studies of neutral material in the interstellar medium were based on a handful of strong resonance lines of trace species that happened to fall at convenient wavelengths in the optical spectral region, notably the Ca II H and K ($\lambda\lambda$3933, 3966) and Na I D ($\lambda\lambda$5889, 5895) lines (Strömgren 1948; Münch 1968). These lines, along with optical resonance lines of several other neutral species, also provided the original key evidence for mass outflows from red giants (Deutsch 1956, 1960). However, until sensitive detectors for high-dispersion spectroscopy became available, there were no deliberate attempts to use these resonance lines to search for neutral material associated with planetary nebulae. The first successful detection of Na I features closely associated with a planetary nebula, as opposed to arising from foreground interstellar material, was accomplished only a few years ago (Dinerstein & Sneden 1988; hereafter DS). In the present paper, we present the results of a follow-up survey of a larger sample of planetary nebulae in the region of the Na D lines.

2. PROPERTIES OF THE SAMPLE

The primary selection criteria for the planetary nebulae in our study were (1) a bright optical continuum; (2) a favorable radial velocity; and (3) detections in other indicators of neutral or molecular material. We observed 21 objects which met at least two of the above criteria, including some that met only two of the three. The requirement of a bright optical continuum, essential for detecting absorption lines, usually meant choosing nebulae with visually bright central stars (Table 1). This criterion obviously can select *against* nebulae with large amounts of associated neutral material and consequent high extinction toward the central stars. To counter this selection effect, we also observed a few nebulae in which the continuum is mainly due to high–surface-brightness recombination emission from the ionized gas: NGC 7027 and NGC 6302, in which the optical continuum is essentially all nebular, and NGC 6790 and IC 4997, in which nebular emission also contributes substantially to the observed continuum. Note that the relative contributions of the star and the ionized gas to the optical continuum are not well known in all cases. For high–surface-brightness nebulae, the nebular component interferes with

[1] Current address: Physics Department, Stanford University, Stanford, CA 94305.

TABLE 1

CANDIDATE NEBULAE AND OBSERVING LOG

Nebula (1)	PK Number (2)	V (central star) (3)	Date (4)	Observatory (5)	Int. (min) (6)	Divisor (7)	Conditions (8)
NGC 40	120+09	11.8[a]	1989 Jan 15	McD	75	α Leo	5″ seeing
NGC 1514	165−15	9.4[b]	1989 Jan 15	McD	60	α Leo	5″ seeing
IC 418	215−24	10.2[c]	1987 Nov 11*	McD	30	...	Clear, 1″ seeing
			1989 Jan 15	McD	90	α Leo	5″ seeing
IC 2149	166+10	11.6[b]	1989 Jan 16	McD	90	β CMa	Thin clouds, 2″ seeing
NGC 2392	197+17	10.5[b]	1989 Jan 15	McD	90	α Leo	5″ seeing
IC 3568	123+34	12.3[b]	1988 Jun 6	McD	90	α Vir	Clear, 1″.5 seeing
			1989 Jan 15	McD	90	α Vir	5″ seeing
			1989 Jan 17*	KPNO	90	α Sgr	Clear
IC 4593	25+40	11.3[b]	1988 Jun 3	McD	90	α Vir	Clear, windy
Sn 1	13+32	14.7[b]	1989 Jun 18	KPNO	90	λ Aql	Moonlight, cirrus
NGC 6210	43+37	12.9[b]	1988 Jun 6	McD	90	α Vir	Clear, 1″.5 seeing
			1989 Jun 19*	KPNO	90	η UMa	Thin cirrus
NGC 6302	349+01	n/a	1989 Jun 18	KPNO	90	λ Aql	Moonlight, high X
NGC 6543	96+29	11.3[b]	1988 Jun 6	McD	90	α Vir	Clear, 1″.5 seeing
NGC 6572	34+11	12.9[c]	1988 Apr 24	McD	60	α Vir	Clear
Sw St 1	1−06	11.8[a]	1989 Jun 17	KPNO	60	σ Sgr	Moonlight, cirrus
NGC 6790	37−06	16:[a]	1988 Jun 8	McD	90	α Vir	Clear, 2″ seeing
			1989 Jun 18*	KPNO	90	λ Aql	Moonlight, cirrus
Vy 2-2	45−02	14.5[c]	1988 Jun 8*	McD	90	α Vir	Clear, 2″ seeing
			1989 Jun 19	KPNO	68	ζ Aql	Moonlight, cirrus
BD +30°3639	64+05	10.2[a]	1988 Apr 24	McD	60	...	Clear
			1988 Jun 4	McD	30	α Vir	Clear, 2″ seeing
			1989 Jun 17*	KPNO	45	σ Sgr	Clear
NGC 6826	83+12	10.7[b]	1989 Jun 17	KPNO	50	σ Sgr	Clear
IC 4997	58−10	14.3[a]	1988 Jun 4*	McD	90	α Vir	Clear
			1989 Jun 19	KPNO	55	ζ Aql	Thick cirrus
NGC 7009	37−34	12.6[d]	1988 Jun 6	McD	40	α Vir	Clear, 1″.5 seeing
NGC 7027	84−03	16.2[e]	1988 Aug 19	McD	60	α Peg	Clear, 1″.5 seeing
Hb 12	111−02	12.7[a]	1988 Oct 28	McD	90	λ Per	Clouds

NOTE.—In cases of multiple observations of an object, the symbol * indicates which spectrum is shown in the figures and was used to measure the line parameters.

[a] Acker et al. 1982.

[b] Shaw & Kaler 1985.

[c] Shaw & Kaler 1989.

[d] Mendéz et al. 1988.

[e] Jacoby 1988; Heap & Hintzen 1990.

determinations of the central star magnitude and makes this a challenging task (see Shaw & Kaler 1985, 1989).

The radial velocity criterion addresses the problem that foreground interstellar absorption can be confused with, or even completely mask, intrinsically nebular features. We tried to minimize this problem by selecting candidate objects with radial velocities well separated from those expected for interstellar material (ISM) along the line of sight at our spectral resolving power (10 km s^{-1}). Fortunately, since planetary nebulae have a larger velocity dispersion than the ISM, this requirement did not eliminate many candidates. However, the identification of a particular absorption feature as being nebular in origin solely on the basis of velocity coincidence is valid only in a statistical sense. For an individual object it is hard to disprove the possibility of an unlucky coincidence of a foreground cloud with the expected nebular absorption velocity, unless an emission component is present in Na I. The emission component is expected to be centered at the nebular systemic velocity v_{sys}; nebular absorption features will be blue-shifted relative to v_{sys} by the expansion velocity of the Na I layer. Our sample also includes a few objects where the expected nebular absorption features but not the emission features would be masked by interstellar lines, and which meet the other criteria (NGC 6572, NGC 7027).

Finally, as mentioned in § 1, the last decade or so has seen the accumulation of a substantial body of evidence for non-ionized material in planetary nebulae. Most of the observations are of molecules, rather than neutral atomic species. The most successful search methods for molecules in planetary nebulae have been observations of emission in the millimeter-wave lines of CO and the near-infrared quadrupole lines of H_2. Both types of emission were first detected in the bright, atypical object NGC 7027 (Mufson, Lyon, & Marionni 1975; Treffers et al. 1976). Subsequent surveys have yielded detections of about 20–30 objects with each technique; compilations are given by Zuckerman & Gatley (1988), Rodríguez (1989), Huggins & Healy (1989), and Huggins (1992, 1993). A handful of planetary nebulae also produce OH maser emission (Sequist & Davis 1983; Payne, Phillips, & Terzian 1988).

Early attempts to detect 21 cm H I lines from planetary nebulae were unsuccessful, probably due to beam dilution and consequent confusion by line-of-sight emission (Knapp 1985). In the last few years, the use of instruments with smaller effective beams has finally yielded a number of definite detections of atomic material in planetary nebulae (Schneider et al. 1987; Taylor et al. 1990). The most interesting cases are those such as IC 418, where both absorption and emission are seen. This allows the calculation of an H I "spin" temperature (Taylor &

Pottasch 1987; Taylor, Gussie, & Goss 1989). In IC 418, the value is of order 1000 K, which may seem surprisingly high. However, this is actually quite consistent with models of photodissociation regions or PDRs (Tielens & Hollenbach 1985; Tielens 1993), which predict the chemical and thermal equilibrium of a molecular cloud illuminated by a strong source of UV radiation.

The gas in the "dissociation zone" between the ionized gas and the predominantly molecular gas cools primarily through emission in far-infrared lines such as [C II] 157 μm and [O I] 63 μm. Over the last decade, these lines have been observed in many interstellar environments. (Their detection requires a space or stratospheric platform, since terrestrial water vapor absorbs strongly at these wavelengths; most of this work has been done from NASA's Kuiper Airborne Observatory.) The first planetary nebula in which these lines were seen was NGC 7027 (Melnick et al. 1981; Ellis & Werner 1984). The 63 μm line has now been detected in over a dozen planetary nebulae, and the trio of lines [C II] 157 μm and [O I] 63, 145 μm, has been measured for several nebulae (Dinerstein et al. 1985, 1995a; Dinerstein 1991, 1995). The observed line strengths indicate high temperatures and densities for these regions ($T \geq 500$ K, $n \geq 10^4$ cm^{-3}). Use of these lines to derive a total mass for the neutral envelope is complicated by the often carbon-rich composition of the planetary nebula material, which differs from the standard, oxygen-rich, interstellar composition profile assumed in the PDR model calculations. However, if it is valid to simply scale the models by the C/H ratio, which is measured for the planetary nebulae in the adjacent ionized material, one finds that the warm photodissociation zones in the planetary nebulae contain one to a few tenths of a solar mass (see references above).

To summarize, the nebulae that we observed at Na I represent a heterogeneous sample. Many, but not all, have been detected in one or more of the tracers discussed above: CO, H_2, H I, or [O I]. By observing Na I in nebulae which have other indicators of neutral and molecular material, we can compare results from these different tracers, and attempt to understand the thermal and ionization structure of the neutral envelope and constrain its overall properties. By including some objects not previously detected in any neutral or molecular line, we explore and exploit the potential of the Na I lines as a sensitive new method for finding additional planetary nebulae with circumnebular neutral material.

3. OBSERVATIONS AND REDUCTIONS

3.1. *McDonald Observatory Coudé Observations*

The observations were obtained with high-dispersion CCD spectrometers on two telescopes, the 2.7 m reflector of the University of Texas McDonald Observatory and the 4 m reflector at Kitt Peak National Observatory. At McDonald Observatory, we used the Tull coudé spectrograph with a 1200 line mm^{-1} grating in first order, and an 800 × 800 pixel Texas Instruments CCD detector. The observations were taken during the period 1986–1989 (see Table 1 for a log of the observations). The spectral coverage was approximately 50 Å, centered on the Na I lines. This spectral segment includes the He I 5876 Å recombination line, which is useful for establishing both the central velocity and the expansion velocity of the ionized gas. The typical spectral resolution element of 2.5 pixels corresponded to 0.20 Å = 10 km s^{-1}. We used a slit width of 0.″5 on the sky, matched to the spectral resolution, and a decker length of 28.″8. The data were binned on-chip by a factor of 4 in cross-dispersion, corresponding to spatial elements of length 0.″6 each. Integration times ranged from about 30 to 90 minutes, and sky conditions varied from clear to light cirrus (Table 1). For each observing run we averaged several dark frames of similar duration to the observations (30–90 minutes) to determine the dark count rate. We then corrected the data for the dark count by subtracting a single constant value per frame rather than by subtracting the average dark frame directly, because of the presence of cosmic-ray hits in the dark exposures. The geocentric wavelength scale was established from FeNe and sodium calibration lamps. We also observed broad-lined hot stars with no intrinsic stellar or interstellar Na I lines, which were used to correct for telluric absorption.

We used IRAF for the bias level and dark count corrections, flat fielding, and the extraction of one-dimensional spectra from the two-dimensional data. The dimensions of the extraction apertures depended upon seeing and the nebular size relative to the slit/decker (e.g., whether the nebula filled the slit, whether the edges of the decker represented the true sky background). For the "on-star" spectra, typical cross-dispersion aperture widths were 4–5 pixels or 2″–3″ (slightly larger than the seeing). We also extracted two parallel "off-star" spectra, positioned symmetrically on either side of the central star, to look for spatially offset nebular Na D emission, as is seen in BD +30°3639 (DS). Sometimes the telluric emission in the Na D lines was readily apparent, at zero geocentric velocity and filling the decker; in other cases it was relatively weak. (The strength of the telluric Na D lines is highly variable with time, both seasonally and during a given night.) However, this telluric emission rarely interfered with the search for nebular features, since the latter were usually located at substantially different positions due to their velocity shifts.

3.2. *KPNO Observations*

Additional observations, including some repeat observations of nebulae previously observed at McDonald Observatory, were obtained during a five night observing run with the Cassegrain echelle spectrograph on the KPNO 4 m in 1989 June. The detector, CCD TI2, was similar to the one used at McDonald Observatory. At KPNO, a 4 s quartz lamp "flash" integration was taken before each science exposure, to increase the CCD sensitivity. We used the "UV-fast" camera, echelle grating 79–63°, and cross-disperser grating 226-1 in first order (Willmarth 1988). The slit width of 0.″75 on the sky corresponded to a resolution element of 2 pixels or 0.20 Å, the same as for the McDonald observations; the decker was 15″ long in the spatial dimension. The Na I lines fell in order 38, and in principle portions of up to 10 additional orders fell simultaneously on the chip. However, we blocked most of the shorter wavelengths with an OG 550 cut-on filter, to avoid scattered light from extremely strong nebular emission lines such as Hβ and [O III] $\lambda\lambda$4959, 5007. For the same reason, we positioned the spectra so that Hα did not fall on the detector. Because the free spectral range (about 150 Å) exceeded the chip width by about a factor of 2, spectral coverage was not continuous. Sections of eight orders between 5300 Å and 6440 Å were recorded, with the bluest orders suffering some attenuation. The absolute wavelength scale was established with a ThAr lamp (Willmarth 1987), and we again observed hot stars with little or no Na absorption, usually trailed, to use for correcting the spectra for telluric H_2O absorptions.

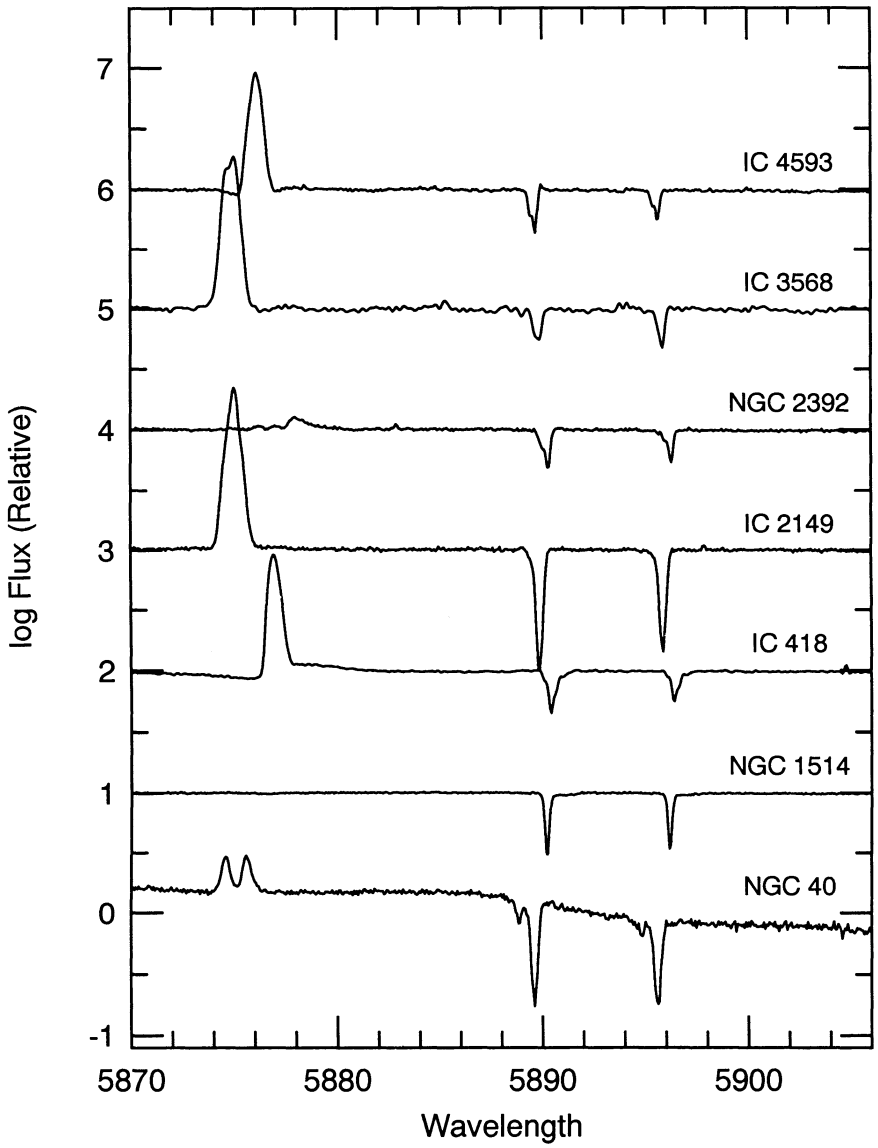

FIG. 1.—Sections of the spectra of seven planetary nebulae, including nebular He I 5876 Å emission lines (near left edge) and the region of the Na I D lines (5889, 5895 Å). The vertical scale is logarithmic. The most prominent Na I absorptions are due to foreground interstellar clouds (see text).

Several initial data reduction steps were conducted at the telescope. At the beginning of each night, 20 short bias frames were taken, averaged, and subtracted from all subsequent exposures. Dark frames were constructed from a median-filtered average of five 90 minute dark exposures, scaled to the appropriate integration times, and subtracted from the data. In reading out the CCD, we binned by a factor of 2 in cross-dispersion, corresponding to 0.″8. Unfortunately, since we aligned the decker precisely along columns in order to preserve spatial information, the spectra displayed a substantial tilt with respect to rows (e.g., 30 pixels vertical shift across 800 pixels or 80 Å). As a result, our coarse binning along the slit caused some difficulty in rectifying the spectra, due to interpolation problems. However, these problems had little effect on the final one-dimensional spectra; they limited our ability to extract narrow apertures, but this resulted in little loss of information since the signal-to-noise ratio per line did not warrant such extractions.

The data were then divided by a flat-field lamp, and one-dimensional spectra were extracted for each nebula. As for the McDonald data, we extracted three spectra: an "on-source" spectrum containing all of the pixels with significant continuum signal; and two adjacent "off-source" spectra containing virtually no continuum signal, to be examined for evidence of emission components. The aperture widths were typically 5–5.5 pixels (about 2″) in the cross-dispersion direction, but were individually tailored to each exposure.

3.3. *Correction for Telluric Features*

The one-dimensional spectra from both observatories were processed further using the SPECTRE reduction package (Fitzpatrick & Sneden 1987). The wavelength solution was done at this stage, as was division by a hot star spectrum to remove the telluric absorption features, primarily due to H_2O. The depths of the strongest telluric features in the divisor spectrum were matched to those in the program object by adding a

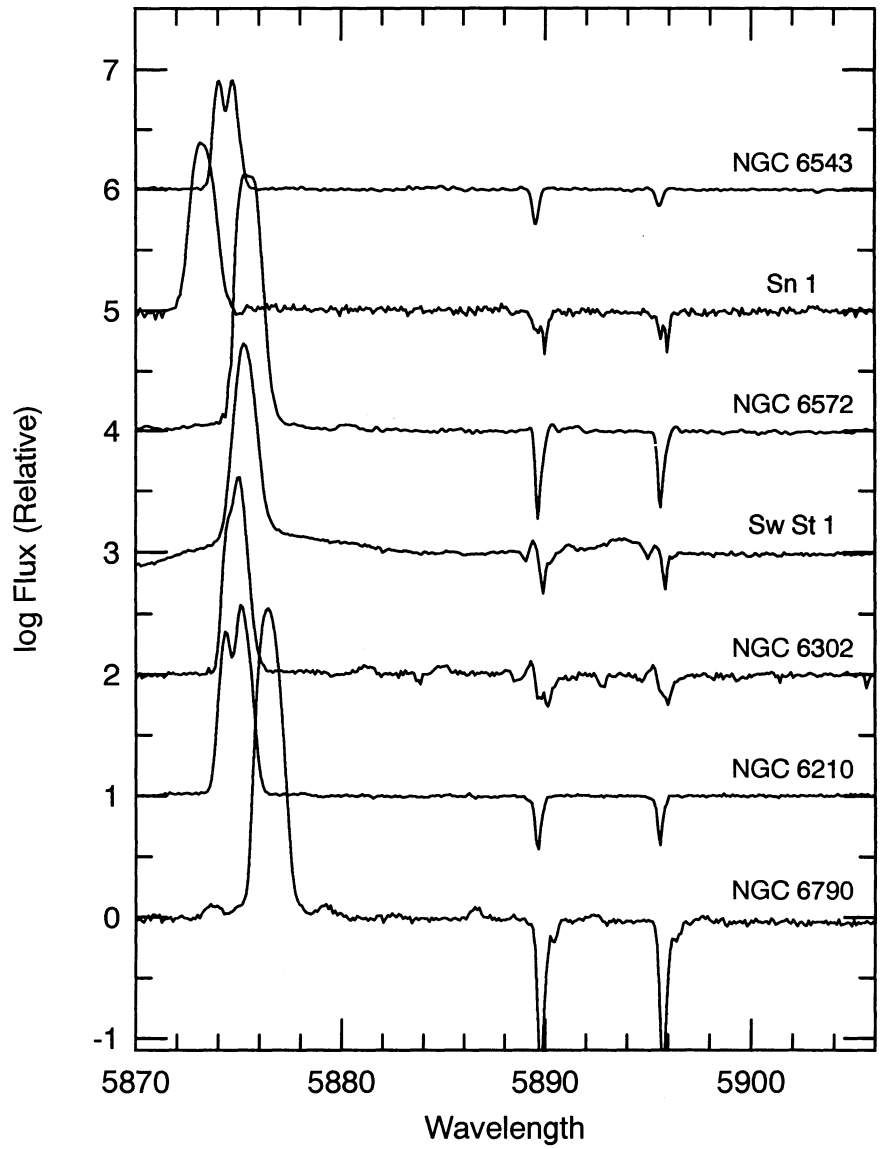

FIG. 2.—Same as Fig. 1, for seven additional nebulae

diluting continuum, before the division was performed. This empirical approach seemed justified in view of the fact that this procedure appeared to remove most of the telluric features in the portion of the spectrum away from the D lines; linear scaling of line strengths is inappropriate because many of the telluric features are strongly saturated. We did not attempt to subtract "sky" spectra in order to remove the telluric Na I emission, which was generally faint compared to the continuum level and at a different velocity than the features of interest. After division, spectra with relatively low signal-to-noise ratios were smoothed with a Fourier filter with a cut-off at spatial frequencies only slightly wider than the resolution element.

3.4. *Measurement of Spectral Features*

The portions of the reduced "on-star" spectra that contain all of the spectral features of interest are shown in Figures 1–3. Here we use a logarithmic vertical scale so that both the strong emission and absorption features can be seen simultaneously. The spectra are dominated by the He I 5876 Å emission line, which shows a variety of profile shapes, and the Na I absorption lines. The deepest Na I features are generally interstellar in origin; some show partially resolved velocity structure. Several planetary nebulae (NGC 40, Sw St 1, IC 4997, and BD + 30°3639) show distinct nebular absorption features even on this highly compressed scale.

Several of the objects also exhibit broad undulations due to stellar features, notably Sw St 1 and BD +30°3639, both of which have Wolf-Rayet type central stars. (Note, however, that the continuum drop across the Na I lines in NGC 40 may be an instrumental effect.) NGC 6302 and NGC 7009 have weak intrinsic continua and were observed through cirrus; these observations are probably contaminated by scattered moonlight. NGC 7027 shows several additional weak nebular emission lines, due mainly to He II (Aller & Keyes 1988).

In Figures 4–6, we replot the region of the Na I features on an expanded, linear scale. In cases where the continuum is sloped or has structure, the data have been divided by a

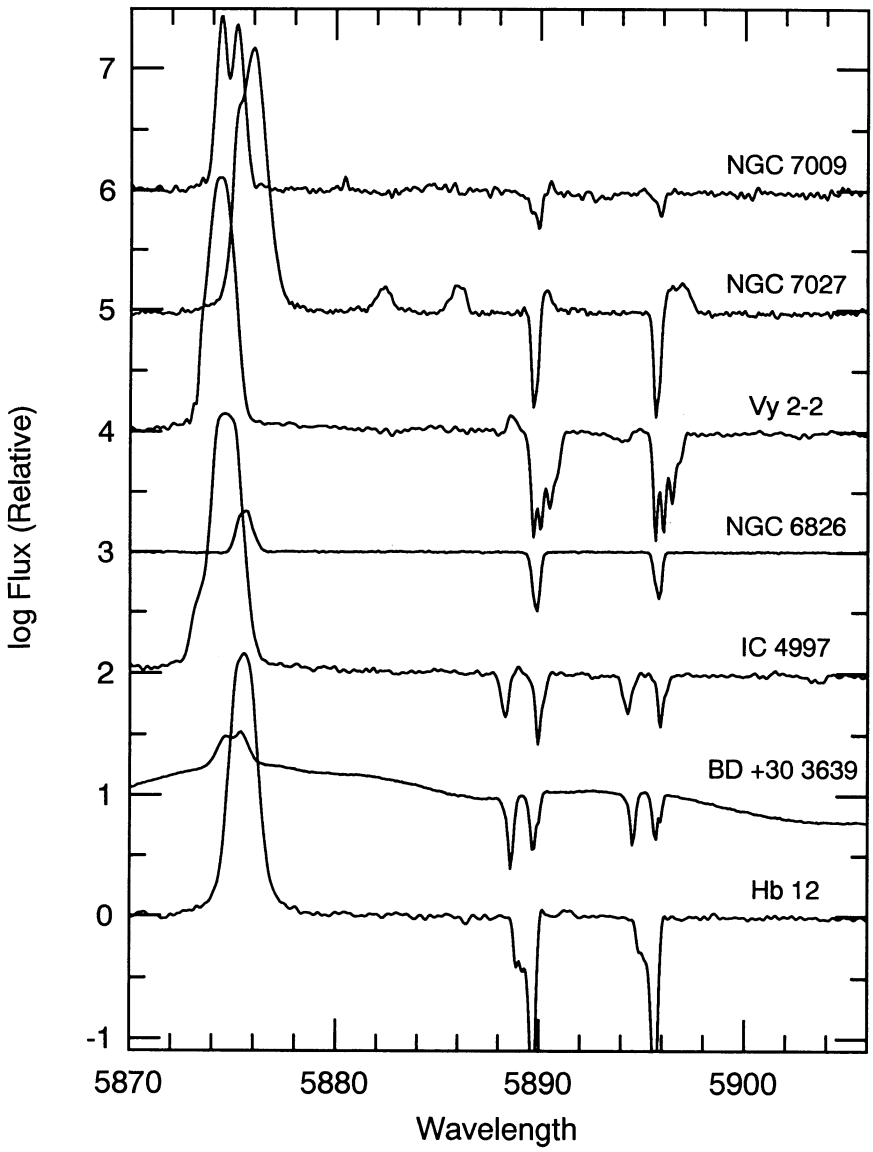

FIG. 3.—Same as Figs. 1 and 2, for seven more nebulae. The Na I lines appear "doubled" in IC 4997 and BD +30°3639; in both cases, the blueward component of each line is due to circumnebular material. Vy 2-2 and Hb 12 show wide, complex, and heavily saturated Na I absorptions due to foreground material.

smooth spline fit to the continuum in order to flatten and normalize the spectra, so broad stellar features seen in Figures 1–3 may not be apparent in Figures 4–6. These figures show the Na line components and profiles in much more detail. Arrows indicate two wavelengths of interest for each Na I line: the solid line indicates the wavelength corresponding to the nebular central velocity, and the dashed line indicates the expected wavelength of any nebular Na I absorption feature. In measuring line velocities, we assumed that the intrinsic wavelengths of the Na I lines were 5889.950 and 5895.924 Å (Morton & Smith 1973). The central wavelengths were measured by methods appropriate to the particular observed line profile: half-power points for symmetric lines, and lowest minima for highly asymmetric features such as some of the interstellar Na I absorption lines. All reported velocities are heliocentric. The determination of equivalent width was also tailored to the spectral shape of each feature. Where the line profiles looked symmetric, we fitted Gaussian absorption profiles to the continuum-normalized spectra. For asymmetric or complex profiles, we simply integrated the area under the continuum. Comparison of the two methods for a given line yielded excellent agreement (less than the stated uncertainties).

4. OBSERVED SPECTRAL FEATURES

4.1. He I 5876 Å *Emission Lines*

Nebular He I 5876 Å emission (intrinsic wavelength 5875.63 Å) is seen in all cases except NGC 2392 and NGC 1514. Some of the He I lines show the double-peaked profile characteristic of a thin, expanding shell (e.g., NGC 40). In other cases the lines are centrally peaked. These nebular emission lines provide a measurement or check of the systemic or central nebular velocity, as well as a species-specific measurement of the expansion velocity in the ionized gas. He I expansion velocities are not generally available in the literature; planetary nebula expansion velocities are usually measured from H I

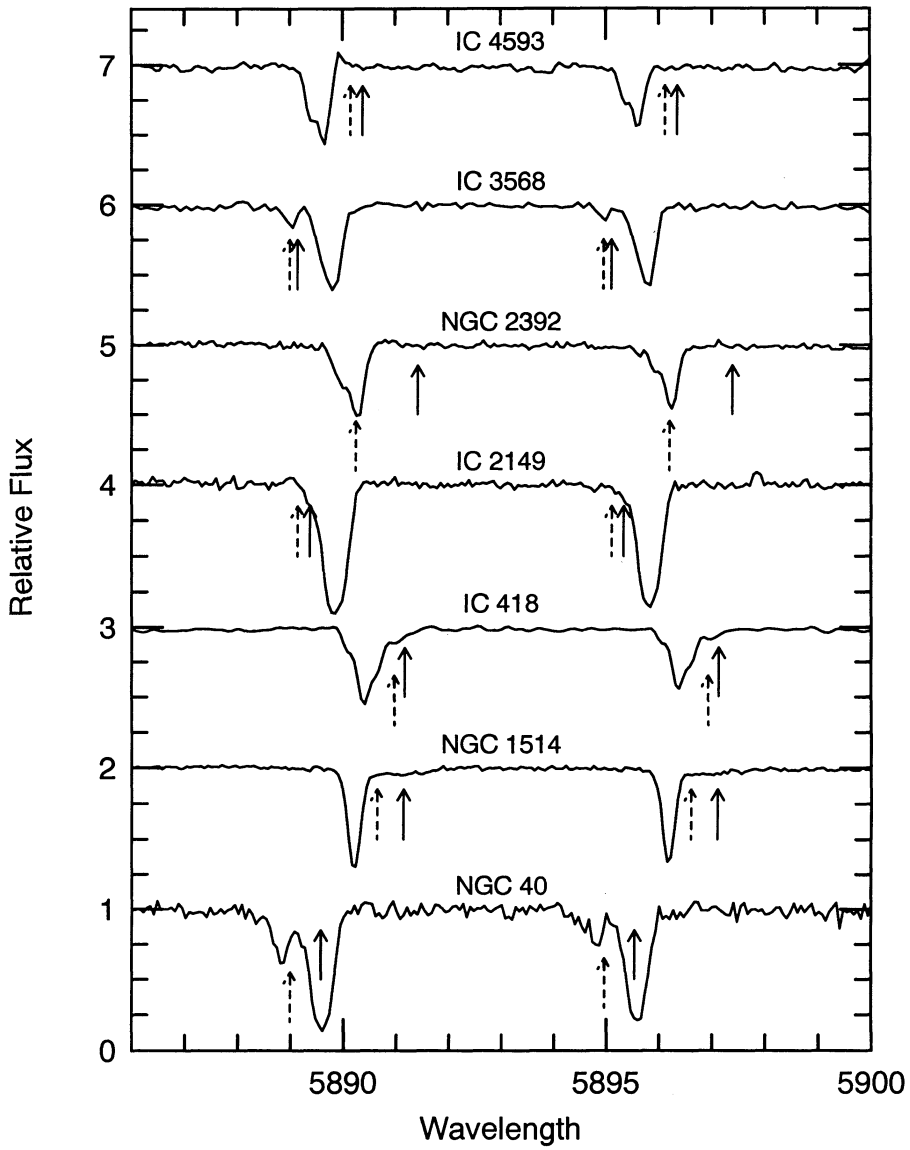

FIG. 4.—Expanded plots on a linear scale are shown for the region of the Na I lines, for the nebulae displayed in Fig. 1. Solid arrows indicate the systemic nebular velocity for each nebula; dashed arrows indicate the blueshifted velocity corresponding to the expanding shell of ionized gas. Nebular Na I absorptions should appear at or near the dashed arrows. Such features are seen in IC 3568, IC 418, and NGC 40.

lines, or from [O III], [O II], or [N II] lines. This is relevant because it has been claimed that expansion velocities determined from different lines in the same nebula show systematic differences; specifically, lower ionization species show larger expansion velocities, e.g., v_{exp}(N II) > v_{exp}(O III) ≈ v_{exp}(H I) (Weinberger 1989a, b).

BD +30°3639, Sw St 1, IC 418, and possibly NGC 2392 show underlying broad emission in He I 5876 Å, arising in the central star. These features are easier to see in Figures 4–6 than in Figures 1–3, unless they have been removed by continuum division. For IC 418, we attribute the apparent offset between the continuum level just shortward and longward of the nebular He I line to stellar P Cygni structure. The nature of the He I features in NGC 2392 is not clear. Perhaps they are residual structure produced by partial cancellation of stellar absorption and emission; alternatively, they may be multiple nebular emission components. The latter is plausible for this particular nebula, which has an unusually complex velocity field (O'Dell & Ball 1985; Gieseking, Becker, & Solf 1985).

In Table 2 columns (2) and (3), we compare the systemic nebular velocities measured from our He I lines with velocities from the catalog of Schneider et al. (1983), who compiled all available values from the literature and calculated a weighted-average "best" value for each nebula. However, the quality of this average varies from object to object. For bright, well-studied objects it is likely to be accurate to a couple of km s^{-1}; but for objects with only one source, the accuracy is only as good as that particular measurement. This must be considered when evaluating the agreement between the two columns. In general, our He I central velocity agrees well with the catalog value, to within our resolution element or better. The exceptions are NGC 2392, Sn 1, and IC 4997. For NGC 2392, as we have already pointed out, the He I line profile is complex and uncertain; the value in Table 2 is the velocity of the brightest individual peak, which may or may not be representative of the true central velocity. The discrepancy of nearly 40 km s^{-1} for Sn 1 is not too worrisome, since the literature value for this planetary is a single unpublished measurement by Mayall;

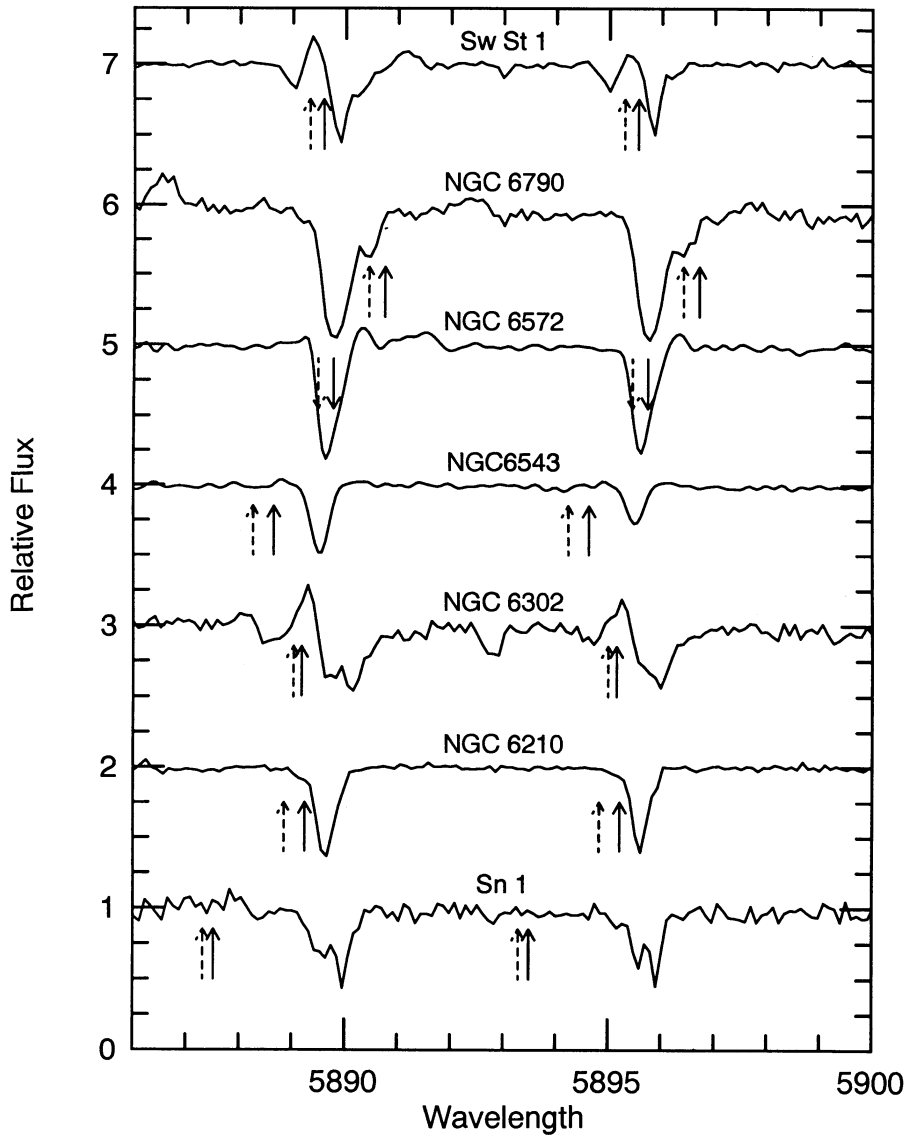

FIG. 5.—Same as Fig. 4, for the nebulae in Fig. 2. Note that the vertical order is different here than in Fig. 2, in order to optimize the display. Nebular Na I absorptions are seen for NGC 6790, Sw St 1, and NGC 6302; the last two also show emission components.

Schneider et al. find that other values from this study are uncertain by 20–30 km s^{-1}. The discrepancy of 17 km s^{-1} for IC 4997 is harder to explain, but might be related to its distinctly asymmetrical He I line profile.

In Table 2 columns (8) and (9), we compare our He I expansion velocities with published expansion velocities. The He I values were measured from the outer half-power points of the line profiles, whether single- or double-peaked, and corrected for an instrumental resolution of 10 km s^{-1}. The literature values are mostly from Weinberger's (1989a) catalog and are measured from [O III] lines. There is a tendency for our He I expansion velocity to be larger than the [O III] value. The only exception to the inequality v_{exp}(He I) $\geq v_{exp}$(O III) is NGC 7027, which has a complex geometry and substantial internal extinction, as does NGC 6302. Excluding these two objects, the nominal mean velocity difference for our sample is $\langle v_{exp}(\text{He I}) - v_{exp}(\text{O III})\rangle = 8.1 \pm 5.0$ km s^{-1} (1 σ). It is not clear whether this represents a real difference, however, given the large scatter and the fact that our moderate-resolution spectra are not optimal for measuring expansion velocities of such narrow features. Furthermore, the [O III] velocities are very heterogeneous, having been measured by various authors using different methods and instruments. A true differential measurement of the He I and [O III] expansion velocities would require a more uniform data set and the use of a consistent measurement technique.

4.2. *Interstellar* Na I *Absorption Features*

The strongest Na I features in our spectra (see Figs. 1–6) are interstellar, near zero velocity with respect to the local standard of rest. These features have central depths ranging from 0.3 (70% residual intensity to greater than 0.9 (< 10% residual intensity). Their profiles suggest the presence of poorly resolved or unresolved multiple velocity components. This is not surprising, since both the thermal width of an interstellar Na I line at 80 K, 0.24 km s^{-1}, and the typical turbulent width of 1–3 km s^{-1} (e.g., Welsh, Vedder, & Vallerga 1990), are much smaller than our spectral resolution element. Also, since the

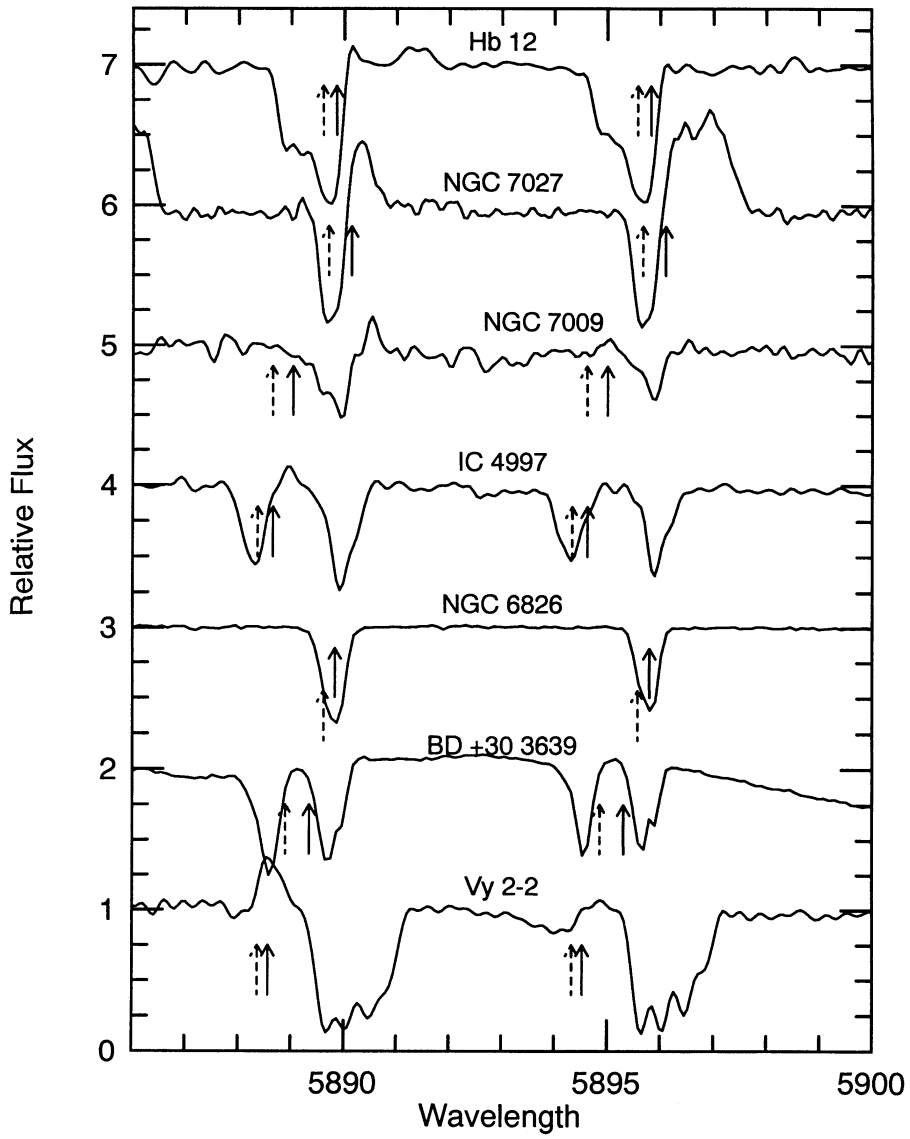

FIG. 6.—Same as Fig. 5, for the nebulae in Fig. 3. Again the vertical order has been changed for display purposes. The strong nebular Na I absorptions in IC 4997 and BD +30°3639 are seen more clearly, as are Na I emission features in NGC 7027 and Vy 2-2. There is also evidence for weak 5895 Å emission in IC 4997, and weak nebular Na I absorptions in Vy 2-2.

distances of the planetary nebulae are of order 1–3 kpc, along lines of sight at rather low galactic latitudes (see Table 1 col. [2]), there is a relatively long path length through the galactic plane; one therefore expects to find multiple velocity components (clouds, or spiral arms) along the path (Vy 2-2 and Hb 12 are the most striking cases). In general, the velocities of our interstellar Na I features match up well with the corresponding components in H I, as observed by Gathier, Pottasch, & Goss (1986), Schneider et al. (1987), and Taylor et al. (1990), although we have not attempted a detailed comparison.

The deep central depths, large equivalent widths, and near-unity ratio of the equivalent widths of the two lines (Table 3) show that the interstellar lines are heavily saturated. Therefore, we did not attempt to determine optical depths and column densities, but instead present only a few quantitative characteristics. In Table 2 column (5) we give the velocity of the lowest minimum of the line profile. (The reader can estimate the approximate velocities of other components from Figures 4–6.) The equivalent widths, given in Table 3 columns (2) and (3), were measured by area integration, and range from about 200 mÅ to over 1 Å.

4.3. "*Nebular*" (*Circumstellar*) Na I *Features*

The main goal of this investigation was to search for Na I features associated with the planetary nebulae, akin to the features previously found in BD +30°3639. The expected locations of circumstellar lines are marked in Figures 4–6. For each line, the solid arrow is positioned at the systemic velocity of the nebula, where nebular emission components should appear if present (DS). The dashed arrow indicates the blueshifted "near-side" velocity of the expanding shell, calculated by subtracting the expansion velocity from the systemic velocity. This is the expected location of any circumstellar Na I absorption if the Na I layer is expanding at the same velocity as [O III]. Since there is no guarantee that the last assumption is strictly true, small deviations from this location are not a reason to

TABLE 2

VELOCITIES OF SPECTRAL FEATURES

Nebula (1)	v_{sys}[a] (Literature) (2)	v_{sys}[b] (He I) (3)	Type of Na Feature (4)	$v_{Interstellar}$ (5)	$v_{Circumstellar}$ (6)	Δv (Circumstellar System) (7)	v_{exp}[c] (Literature) (8)	v_{exp} (He I) (9)
NGC 40	−20	−29	Absorption	−17	−56	−36	29	35[d]
NGC 1514	+60	...	None	+13	...	...	25	
IC 418	+62	+66	Absorption	+23	+54	−8	10[e]	11
IC 2149	−31	−30	None	−3	...	...	10	25
NGC 2392	+75	+114:[f]	None	+17	...	...	60	
IC 3568	−41	−42	Absorption	−7	−48	−7	8	20
IC 4593	+22	+24	None	−15	...	...	12	11
Sn 1	−87:[g]	−124	None	0	...	...	10	23
NGC 6210	−36	−38	None	−17	...	...	20	32[d]
NGC 6302	−39	−35	Emission[h]	+5	−34	+5	8	16
			Absorption[h]		−68	−29		
NGC 6543	−66	−65	None	−22	...	...	20	27[d]
NGC 6572	−8	−9	None	−16	...	...	15	23
Sw St 1	−19	−20	Emission	−3	−27[i]	−8	13	16
			Absorption		−47	−27		
NGC 6790	+40	+40	Absorption	−8	+24	−16	15	17
Vy 2-2	−71	−64	Emission	+5	−69[j]	+2	10[k]	20
			Absorption		−110	−39		
BD +30°3639	−31	−30	Absorption	−13	−69	−38	23	40[d]
NGC 6826	−6	−4	None	−6	...	...	11	17
IC 4997	−66	−49	Emission	−1	−51[j]	+15	15	27
			Absorption		−83	−17		
NGC 7009	−47	−43	None	0	...	...	20	28[d]
NGC 7027	+9	0	Emission	−13	+19	...	22	14[l]
Hb 12	−5	−7	None	−12	...	...	13	20

[a] Heliocentric systemic velocity, from Schneider et al. 1983.
[b] Measured from our He I 5876 Å line.
[c] From Weinberger (1989a), unless otherwise indicated; values measured from [O III] lines.
[d] Measured from the outer half-power points of a double-lined profile (see figures).
[e] Bianchi & Falcetta (1988).
[f] Very asymmetric profile; FWHM indeterminate.
[g] From Perek-Kohoutek (1968), citing an unpublished measurement by Mayall.
[h] Had to divide out a deep adjacent interstellar feature.
[i] Eaten away by interstellar absorption on the red edge.
[j] From 5889 Å line only.
[k] Miranda & Solf (1991).
[l] Does not include blue wing.

reject a line as circumstellar in origin. On the other hand, features located far from the expected velocities are unlikely to be associated with the nebula. However, if such features are present at the same velocity in both Na I lines and show a plausible equivalent width ratio (between 1 and 2), then they are probably real absorptions from unrelated foreground material; the fact that the Na I lines are a doublet provides a built-in redundancy that should screen out random noise spikes or instrumental defects such as bad pixels.

The types of nebular features seen in each nebula (absorption, emission, both) are listed in column (4) of Table 2, and their radial velocities are reported in column (6). In column (7), we calculate the differential velocities $\Delta v = v_{Circumstellar}(\text{Na I}) - v_{sys}$. When measured from absorption lines, this should be the effective expansion velocity of the Na I layer, to be compared with expansion velocities measured from emission lines of other species (cols. [8] and [9]). As remarked in § 4.1 above, differences in measurement techniques may well produce spurious differences even among velocities that are all measured from emission lines. This might be even more true when comparing velocities measured from absorption lines, which sample a pencil beam (against the central star continuum), with those measured from emission lines, which represent an emissivity-weighted integral over the portion of the nebula entering the slit. In principle, it seems likely that circumstellar absorption lines will be biased toward higher blueshifts than the emission lines, even leaving aside the possibility of stratification. Furthermore, for nebulae with nonspherical kinematics, such as bipolar structure with higher expansion velocities along the polar axis than in the "equatorial" plane, orientation effects may produce further differences in the measured expansion velocities.

The equivalent widths of the circumstellar absorption features are reported in columns (4) and (5) of Table 3. The stated measurement uncertainties were estimated from the internal agreement between values measured by Gaussian fitting and by area integration, and from allowance for the admissible range in continuum level. The upper limits are about 10–20 mÅ, depending on the continuum signal-to-noise ratio. The line widths as found from the profile fits were mostly indistinguishable from the instrumental resolution, for weak lines. BD +30°3639 and IC 4997 have wider, heavily saturated nebular absorption lines. NGC 6302, which has high velocity flows and a complex geometry (Meaburn & Walsh 1980), apparently shows circumstellar absorptions wider than the instrumental resolution, but is complicated by the fact that the absorption lines are partially filled in by emission.

The following nebulae show weak to moderately strong circumstellar Na I absorption lines at or near the predicted velocities, but no emission components: IC 3568, IC 418, NGC 40, and NGC 6790. For these objects, the weaker Na I line (5895 Å) has an equivalent width between 20 mÅ (roughly our

TABLE 3

EQUIVALENT WIDTHS AND COLUMN DENSITIES

Nebula (1)	Interstellar Features W_λ(5889 Å) (2)	Interstellar Features W_λ(5895 Å) (3)	Circumstellar Features W_λ(5889 Å) (4)	Circumstellar Features W_λ(5895 Å) (5)	Ratio 5889/5895 Å (6)	τ_0 (7)	log N(Na I) cm^{-2} (8)
NGC 40	460 ± 30	410 ± 30	135 ± 15	75 ± 15	1.8 ± 0.6	0.3	11.9
NGC 1514	210 ± 20	190 ± 20	≤10	≤10	≤2.0	...	≤11.0
IC 418	260 ± 20	205 ± 20	38 ± 4	23 ± 4	1.7 ± 0.5	0.5	11.5
IC 2149	500 ± 20	460 ± 20	≤10	≤10	≤2.0	...	≤11.0
NGC 2392	260 ± 20	180 ± 20	...[a]	[a]	...	...	...
IC 3568	300 ± 10	250 ± 10	39 ± 4	24 ± 4	1.6 ± 0.5	0.8	11.5
IC 4593	235 ± 15	170 ± 15	...[b]	≤10	≤2.0	...	≤11.0
Sn 1	320 ± 20	285 ± 20	≤20	≤20	≤2.0	...	≤11.3
NGC 6210	310 ± 10	250 ± 10	≤15	≤10	≤2.0	...	≤11.0
NGC 6302	360 ± 30	280 ± 30	60 ± 10	30 ± 5	2.0 ± 0.5	0.9	11.5
NGC 6543	205 ± 10	105 ± 10	≤10	≤10	≤2.0	...	≤11.0
NGC 6572	360 ± 15	345 ± 15	≤10	≤10	≤2.0	...	≤11.0
Sw St 1	260 ± 20[c]	155 ± 20[c]	55 ± 15	55 ± 15	1.0 ± 0.6	≥0.5	≥11.8
NGC 6790	610 ± 30	510 ± 30	100 ± 30[d]	100 ± 30[d]	1.0 ± 0.9	≥0.2	≥12.0
Vy 2-2	1175 ± 30	1030 ± 30	...[e]	100 ± 40[e]	...	...	≥12.0
BD +30°3639	320 ± 20	260 ± 20	350 ± 20	280 ± 20	1.25 ± 0.16	3	12.8
NGC 6826	355 ± 15	280 ± 15	≤100[d]	≤100[d]	≤2.0	...	≤12.0
IC 4997	400 ± 15	300 ± 15	270 ± 15	275 ± 30	1.0 ± 0.15	≥8	≥13.0
NGC 7009	295 ± 30	170 ± 30	≤20	≤20	≤2.0	...	≤11.3
NGC 7027	370 ± 20	430 ± 20	...[f]	[f,g]	...	...	...
Hb 12	915 ± 20	890 ± 20	...[f]	[f]	...	...	...

[a] Feature at −14 km s^{-1} relative to 5895 Å, but not seen in the stronger 5889 Å line.
[b] Telluric emission spike.
[c] Interstellar absorption partially filled in by nebular emission at the blue edge.
[d] On the wing of a very strong interstellar line.
[e] Confused by emission components and structure in the continuum.
[f] No information available; masked by strong interstellar absorption.
[g] Adjacent emission line is He II 5896.9 Å.

detection limit) and 80 mÅ, and the equivalent width ratio, $W_\lambda(5889)/W_\lambda(5895) = 2.0$, corresponds to the optically thin or "linear" regime of the curve of growth. Much stronger, deeper, and obviously saturated absorption lines are seen in BD +30°3639 and IC 4997, with W_λ values of 300–400 mÅ and equivalent width ratios of nearly unity. Absorption components are also seen in Sw St 1, NGC 6302, and probably Vy 2-2, but their equivalent width measurements are uncertain due to their close juxtaposition with nebular emission features, which may partially fill in the absorption. For this reason, the fact that Sw St 1 has an apparently saturated ratio of 1.0, while NGC 6302 has an unsaturated ratio of 2.0, is not necessarily significant. Overall, we therefore see evidence for nebular absorption in nine of the 21 observed nebulae.

Emission components in the Na I lines are seen in Sw St 1, NGC 6302, NGC 7027, Vy 2-2, and probably IC 4997. The emission features of BD +30°3639 are not apparent in the KPNO spectrum of Figure 6 (the "on-star" spectrum shown in Fig. 2 of DS has small continuum bumps at the expected emission wavelengths, but only inspection of the "off-star" spectra makes the case convincing). Most of the objects showing emission also have circumstellar absorption features, and show P Cygni-like profiles. NGC 7027 has a radial velocity such that any circumstellar absorption lines would fall behind the interstellar ones, which makes it impossible to unambiguously determine the origin of the observed deep absorption features; however, interstellar absorption will not mask the emission components, which should be shifted in velocity, and indeed, strong emission features are seen at the nebular systemic velocity in both Na I lines. (The reader should not be confused by the "double-hump" profile of 5895 Å line; the redward peak here is He II 5896.9 Å, a line not seen in the other nebulae probably because of their cooler central stars and hence lower degree of ionization.)

The observability of the nebular Na I emission depends on various factors, including the size of the Na I region relative to the slit (i.e., the locus of Na I emission might be located outside our aperture), the surface brightness and line-to-continuum ratio of the Na I lines, and the extent to which nebular emission lines would be unresolved from the terrestrial emission. In the KPNO data there was further interference from an instrumental flaw near 5888.2 Å (−90 km s^{-1}). For Sw St 1, nebular Na I emission lines are seen both in the on-star and off-star spectra, but the off-star spectra for the other nebulae detected at Na I were too noisy to yield conclusive results.

For several nebulae our spectra yield definite nondetections of both absorption and emission lines, while for others we are able to rule out only one or the other of these possibilities, due to their velocities. We can rule out the presence of either kind of feature in IC 2149, IC 4593, NGC 1514, NGC 6543, NGC 6210, Sn 1, and probably NGC 7009. (The emission "blip" on the red edge of IC 4593 is due to imperfect removal of telluric Na I emission.) For IC 2149 and NGC 6828, we can rule out absorption features only. For NGC 2392, we can rule out the presence of nebular emission but not absorption; although the systemic velocity is located far from zero, the high expansion velocity of this object would shift any nebular absorptions that might be present into the interstellar features. Upper limits for the nondetections, in the range 10–20 mÅ, are reported in Table 3.

The radial velocity of NGC 6572 is unfavorable; in this object we would have seen circumstellar absorptions only if they were both strong and blueward of the nominal expansion velocity (however, the latter is the case in BD +30°3639). For

Hb 12 our results are completely indeterminate; this object turned out to show an extraordinarily strong and wide interstellar feature, arising from multiple components along the line of sight. It is not always possible to anticipate the detailed properties of the interstellar features, particularly for objects with poorly known distances. Indeed, this method has been used in reverse: the detection of the various foreground velocity components in the 21 cm H I line is one of several methods for determining the distances of planetary nebulae, for example by Gathier, Pottasch, & Goss (1986).

5. ANALYSIS

5.1. *Nebular Expansion Velocities*

Our Na I expansion velocities were compared with other measurements of expansion velocities in Table 2. For the literature values, taken from Weinberger (1989a), we chose [O III] velocities, since this is the only measurement that is available for every nebula in our sample. Weinberger found that for a given nebula the H I and [O III] velocities usually agree, while the low-ionization species [N II] and [O II] show expansion velocities that are systematically larger by about 4.5 km s^{-1} on the average. He interprets this as being the result of an increase of v_{exp} with radial distance from the central star, together with the effects of ionization stratification (Weinberger 1989a, b). The [N II] lines are presumed to arise in the outer layers of the nebula, which are expanding faster than the inner, [O III]–emitting region due to nonuniform nebular expansion, possibly as a result of acceleration by radiation pressure on grains mixed with the ejected gas. Extrapolating this trend, we might expect the Na I absorption lines, which are presumably formed farther out in the nebular envelope than the [N II] lines, to show even larger expansion velocities.

As mentioned above, our measured He I expansion velocities are slightly larger than the [O III] values, although the apparent systematic difference of 8 km s^{-1} is not statistically significant given the large scatter. Our most reliable Na I expansion velocities are for those objects where the absorption lines are not affected by emission, namely NGC 40, IC 418, IC 3568, and NGC 6790. For the last three, the Na I velocity agrees within 1–2 km s^{-1} with the [O III] expansion velocity. For NGC 40 we find v_{exp}(Na I) = 36 km s^{-1}, which is 7 km s^{-1} larger than the cataloged [O III] velocity; however, note that our own measured He I expansion velocity (measured from the very same spectrum) *agrees* with our Na I value. The same is true for IC 4997, where the absorption features are sufficiently strong that the line center location is probably unaffected by the weak emission features. For this object, again our Na I expansion velocity is larger than the published [O III] velocity (Δ = 8 km s^{-1}), but our Na I and He I expansion velocities agree. In fact, even for BD +30°3639, where the Na I velocity is 15 km s^{-1} larger than the published [O III] value, our Na I and He I velocities agree! The absorption velocities for NGC 6302, Sw St 1, and Vy 2-2 quoted in Table 2 should not be given a great deal of weight, since these absorption features are significantly filled in by reemission (see Figs. 5 and 6); the observations of NGC 6302 and Sw St 1 were also affected by scattered moonlight.

We conclude that so far there is no convincing evidence for Na I expansion velocities substantially larger than the expansion velocities in the bulk of the ionized gas, as measured by [O III] and He I. It must be kept in mind, however, that it would not be possible to establish or rule out systematic differences as small as a few km s^{-1}, given the spectral resolution used for this study (10 km s^{-1}) and the heterogeneity of the literature values. Resolution of this question must await a survey at higher spectral resolution and S/N of a statistically significant sample of nebulae. Nevertheless, we do find it interesting that Taylor et al. (1990), who measured H I expansion velocities from 21 cm absorption lines in five planetary nebulae, also concluded that the expansion velocities of the neutral gas are similar to the expansion velocities in the ionized gas.

5.2. *Optical Depths and Column Densities*

For objects with absorption components, we used the ratio of the equivalent widths of the two Na I lines to deduce τ_0 (5895 Å) and the corresponding column density of Na I, by applying the "doublet-ratio" method (DS). This essentially gives a two-point fit to the curve of growth. In general, the curve of growth depends on the form of the line profile function; our formula is based on equation (2–41) of Spitzer (1968, p. 19), which assumes a single-component, Doppler-broadened line profile. The advantage of this formula over the simpler equation that relates the line center optical depth to column density and Doppler width (Spitzer, eq. [2–40]) is that our approach avoids the need to insert an explicit value for the line width parameter (b or β), which we are unable to measure at our present spectral resolution. Then, following the notation of Spitzer, $C = \tau_0(5895\ \text{Å})$ and $F(2C)/F(C) = W_\lambda(5889)/W_\lambda(5895)$. We list these values in Table 3. The column densities N(Na I), given in column (8), were computed by reading off the values of $F(C)/C$ from Spitzer's Table 2.1 (p. 20), and inserting them into equation (1) of DS.

For objects in which no Na I absorptions were detected, the upper limits on the column densities were computed by assuming the optically thin limit, $F(C)/C = 0.886$, and the upper limits for $W_\lambda(5895)$ given in column (5). For Sw St 1, NGC 6790, and IC 4997, we cite *lower* limits on log N(Na I). In these objects, the equivalent width ratio is nearly unity, indicating that the absorption lines are very optically thick. We therefore took the lowest optical depth values allowed by our error bars, in order to estimate minimum column densities. For Vy 2-2, the nominal equivalent width ratio of the weak, shallow absorption features is unphysical, probably due to filling in by emission; the cited lower limit assumes low optical depth and $W_\lambda(5895)$ = 100 mÅ, and is very uncertain.

Use of the doublet-ratio method may seem simplistic, but has the advantage that the only information it requires is the equivalent widths of the two Na I lines. Nachman & Hobbs (1973) criticized the use of this method for strong interstellar lines, when the velocity field is far from Maxwellian; they showed that a blend of lines due to several different clouds with velocity separations comparable to their widths could be mistaken for a single broad, highly saturated component, leading to a very large error in the deduced column density. However, we regard it as unlikely that the radial profile of the velocity field of the circumstellar Na I in planetary nebulae is strongly bimodal or multiple. It is more likely to be similar to that of ionized gas, strongly peaked with a relatively smooth distribution around the central value. Jenkins (1986) has shown that even if the velocity field is broad, as long as it is reasonably smooth and centrally peaked, the simple method of equivalent width analysis produces column densities accurate to 15% even for fairly high optical depths ($\tau_0 \approx 5$). Therefore, we believe that our simple analysis should yield reasonable estimates for the Na I column densities in the planetary nebulae.

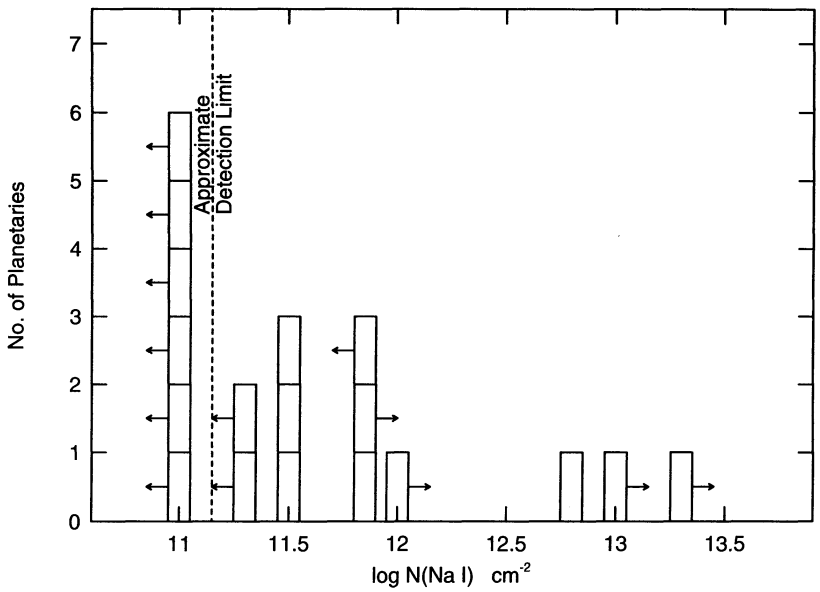

FIG. 7.—Histogram of the derived Na I column densities in planetary nebulae. The upper limits at log N(Na I) = 11.0 and 11.3 correspond to upper limits on the line equivalent widths of 10 and 20 mÅ, respectively, and defines our effective detection limit. Lower limits are shown when the lines are optically thick (see Table 3 and the text).

With higher spectral resolution than employed here, the line profiles could be spectrally resolved and examined in detail, and a more sophisticated analysis might be warranted. Such a treatment would be particularly appropriate for the objects with P Cygni profiles, although most likely one would only be able to define a *range* of allowed envelope properties, rather than a unique set of values. Models for the scattering of resonance lines in expanding spherical envelopes with central cavities show that the emergent line profiles tend to be more sensitive to the form of the velocity field than to the optical depth and the form of the density distribution (Natta & Beckwith 1986). For example, the strength of the emission relative to the absorption component can be strongly affected by the presence and location of acceleration zones (Beckwith & Natta 1987). Information about the spatial brightness distribution of the emission might help disentangle these effects, but would require spectra at multiple spatial positions or very narrow band images. A more realistic approach might be to seek information on the velocity structure from optically thin emission lines arising in the same layers, such as [C II] 157 μm, or to obtain spatially and spectrally resolved observations of the H I 21 cm emission (e.g., Taylor et al. 1989).

5.3. *Comparison to* H I *Results*

A histogram of the Na I column densities is shown as Figure 7; note that some entries are actually upper or lower limits (see Table 3). However, derivation of a column density for Na I does not give a direct measurement of the *total* column density through the neutral shell. For the latter, one needs a value for the ratio N(Na I)/N(H I). In the interstellar medium, this ratio is generally much smaller than the cosmic elemental ratio Na/H = 1.8×10^{-6} (Allen 1973), because less than 1% is in Na I. Since Na I has a very low ionization potential, 5.1 eV, whereas Na II has an ionization potential of 47.3 eV, nearly all of the atomic sodium in the ISM will be singly ionized. Depletion into dust grains apparently only reduces the gas-phase abundance of sodium by a relatively small and uniform factor of ~ 4 (Phillips, Pettini, & Gondhalekar 1984). In contrast to some earlier studies which found a quadratic relation between the interstellar column densities of Na I and H I, Ferlet, Vidal-Madjar, & Gry (1985) found that the linear relation N(Na I)/N(H I) = 8×10^{-10} holds for all lines of sight with moderate extinction and column densities, $A_V \leq 1$ or N(H I) $\leq 10^{21}$ cm^{-2}. (At larger column densities, the hydrogen starts to become molecular.) The intrinsic scatter around this relation is small, and the ratio does not appear to depend on the local density, which primarily affects the ionization balance through the recombination rate.

Several of the nebulae for which we detect Na I absorptions were recently detected in the 21 cm H I line (Taylor et al. 1990 and references therein). For these we can determine N(Na I)/N(H I) directly; the resulting values are given in Table 4. In

TABLE 4

COMPARISON WITH H I RESULTS

Nebula	N(Na I) (cm^{-2})	N(H I) (cm^{-2})	Reference	Ratio (Na I/H I)
NGC 6790.....	8×10^{11}	2.7×10^{20}	1, 2	3×10^{-9}
IC 418	4×10^{11}	2.9×10^{19}	1, 3	1.4×10^{-8}
NGC 6302.....	$\geq 3 \times 10^{11}$	6.4×10^{20}	1, 4	$\geq 5 \times 10^{-10}$
IC 4997	6×10^{12}	3.8×10^{20}	1, 5	1.6×10^{-8}
BD +30°3639.....	5×10^{12}	$0.4–4 \times 10^{20}$	1	$0.1–1.2 \times 10^{-8}$

REFERENCES.—(1) Taylor et al. 1990; (2) Gathier et al. 1986; (3) Taylor et al. 1989; (4) Rodríguez et al. 1985; (5) Altschuler et al. 1986.

general, we find a larger ratio than the interstellar value (for NGC 6302 we have only a weak lower limit). We consider it unlikely that there is a significant contribution to the Na I line from the ionized component of the planetary nebula. Therefore, we conclude that the overall degree of ionization of the neutral material around the planetary nebulae is lower than in the diffuse interstellar clouds. Reasons for this may include more complete shielding from UV radiation, higher local gas densities (which favor recombination), and a contribution to the Na I lines from the region where hydrogen is molecular. A more remote possibility might be a smaller Na depletion factor into grains, since Lenzuni, Natta, & Panagia (1989) have argued that dust may be destroyed in planetary nebulae.

6. DISCUSSION

6.1. *Comparison with Other Indicators of Neutral Envelopes*

It has long been an unsolved question whether planetary nebulae are "matter-bounded" structures, in which the edge of the ionized region coincides with the material boundary, or whether they are ionization-bounded Strömgren spheres, with neutral material beyond the ionized zone. Until recently the evidence in favor of the latter scenario was mainly indirect. Pottasch (1980, 1988) favored the ionization-bounded picture on the basis of an observed correlation between ionized mass and nebular radius. This is consistent with the following evolutionary picture: as time elapses, the nebula expands and the gas density drops, and the stellar UV photons are able to ionize a larger amount of material. In § 2 we reviewed recent, direct evidence for neutral and molecular species in planetary nebulae. We now assess the correspondence between the objects in which we detect nebular Na I and objects detected by other techniques, and compare the utility of the various methods.

As discussed above, the main techniques that have been used to detect neutral and molecular material in planetary nebulae are the H I 21 cm line, far-infrared lines of [O I] and [C II], millimeter-wave CO rotational transitions, and near-infrared H_2 emission. In Table 5, we present a brief score card for the planetary nebulae that we observed in this study. For each technique we list one of three possible entries: a positive detection (Y), a null result from a search (N), or no information (-). In most cases the last choice means that no search has been made, but for Na I it indicates that the nondetection is inconclusive for reasons discussed above. Since the detection thresholds are not uniform among either the techniques or the sources, and some individual objects have characteristics that invalidate certain methods (e.g., an unfavorable radial velocity for Na I or H I), null results are not always conclusive. Furthermore, Table 5 includes only information in the literature or from our own umpublished work, and may be somewhat out of date by the time this paper is published. However, we feel that this compilation represents a useful starting point for putting together a comprehensive overview of these circumnebular envelopes.

Of the columns listed in Table 5, we consider H I and [O I] to be indicators for a "atomic" or dissociated region, and H_2 and CO to be tracers of molecular gas. (We do not include OH maser emission, which has been detected in NGC 6302 and Vy 2-2, since this emission calls for special conditions and has been observed in only a few nebulae.) Note that, while H I and O I are ionized by UV photons of similar energy, the [O I] 63 μm line will be seen only if the gas is relatively warm, whereas the 21 cm line has no such requirement. Furthermore, the infrared H_2 and millimeter-wave CO lines both arise from molecular gas, but CO may be partially or largely dissociated in the regions where the hydrogen is still fully molecular (see the discussion in Bachiller et al. 1988).

TABLE 5

COMPARISON OF NEUTRAL AND MOLECULAR INDICATORS

Nebula	Na I	H I	[O I]	H_2	CO
NGC 40	Y	...	Y (1)	...	N (2)
NGC 1514	N	N (3)	...	...	...
IC 418	Y	Y (4, 5)	Y (1)	N (6)	N (2)
IC 2149	N	N (3)	...	...	N (2)
NGC 2392	...	N (3)	N (7)	...	N (2)
IC 3568	Y	...	...	...	N (2)
IC 4593	N	N (3)	...	N (8)	N (2)
Sn 1	N	...	...	...	...
NGC 6210	N	N (3)	N (7)	N (8)	N (2)
NGC 6302	Y	Y (9, 10)	Y (7)	...	Y (2)
NGC 6543	N	...	N (7)	...	N (2)
NGC 6572	...	N (11)	Y (1)	N (6, 8)	N (2)
Sw St 1	Y	...	...	Y (8)	...
NGC 6790	Y	Y (12, 11)	...	N (6)	N (2)
Vy 2-2	Y	...	Y (7)	Y (8)	N (2)
BD +30°3639	Y	Y (11)	Y (1)	Y (13)	Y (14)
NGC 6826	N	N (2)	...	...	N (2)
IC 4997	Y	Y (15)	...	N (6, 8)	N (2)
NGC 7009	N	...	...	...	N (2)
NGC 7027	Y	N (16)	Y (1)	Y (13, 6)	Y (2)
Hb 12	...	...	Y (7)	Y (13, 17)	N (2)

REFERENCES.—(1) Dinerstein et al. 1991; (2) Huggins & Healy 1989; (3) Schneider et al. 1987; (4) Taylor & Pottasch 1987; (5) Taylor et al. 1989; (6) Zuckerman & Gatley 1988; (7) Dinerstein et al. 1995c; (8) Dinerstein, unpublished work; (9) Rodríguez & Moran 1982; (10) Rodríguez, García-Barreto, & Gómez 1985; (11) Taylor et al. 1990; (12) Gathier et al. 1986, (13) Beckwith et al. 1978; (14) Bachiller et al. 1991, 1992; (15) Altschuler et al. 1986; (16) Pottasch et al. 1982; (17) Dinerstein et al. 1988.

Despite some gaps, the following pattern emerges from an examination of Table 5. Nearly all of the nebulae can be assigned to one of three categories: (I) no evidence for either atomic or molecular material (e.g., NGC 2392, IC 4593, NGC 6210); (II) evidence for neutral atomic gas, but no evidence for molecular gas (e.g., IC 418, NGC 6790, IC 4997); and (III) evidence for both neutral atomic and molecular gas (e.g., NGC 6302, NGC 7027, Hb 12). The exceptions can probably be attributed to sensitivity limitations.

We interpret these categories as a sequence of increasing stratification in the nebular envelope. Group I objects have no neutral material, or very small amounts. Group II objects possess an outer neutral envelope that is photodissociated out to the edge of the mass distribution. Group III objects contain both a photodissociated and a molecular region. This is not necessarily an evolutionary sequence. Undoubtedly individual nebulae can move from one category to another as the nebula expands and becomes more fully ionized, but it is entirely possible that not *all* planetary nebulae will traverse the sequence group III → group II → group I. The progenitors of planetary nebulae have a range of masses, and their central stars have a wide range in luminosity and evolutionary timescale. For example, the objects with molecular layers (group III) may primarily come from more massive progenitors, which expel larger amounts of mass when they produce planetary nebulae. This idea is supported by the correlation of CO detections for a large sample (100 objects) with N/O abundance (Huggins & Healy 1989), since nebulae with elevated N/O are believed to arise from massive stars (i.e., Peimbert & Torres-Peimbert 1983). Another important parameter is the mass-loss rate; a high rate makes it easier for the material to self-shield, which helps the molecules survive. For certain cases the dissociation and ionization fronts may never reach the outer boundary of the ejected envelope, so that the outer layers remain molecular until it merges into the ambient medium (Spergel, Giuliani, & Knapp 1983). These are only a few of the factors that can influence the instantaneous balance between the ionized, atomic, and molecular phases in planetary nebula envelopes.

6.2. *Masses of the Neutral Envelopes*

Column densities alone cannot be used to determine the total mass of neutral material; to do this one needs additional information on the distance and the shell geometry (density and size). On the other hand, estimates based on integrated, optically thin emission lines depend only on distance. Such estimates have been made from H I lines for a only few nebulae. For BD +30°3639, Taylor et al. (1990) detected a spatially compact emission feature in the 21 cm line. They use this line to estimate an H I mass of 0.028 $M_\odot$ for an assumed distance of 0.9 kpc; the value increases to 0.27 $M_\odot$ for a distance of 2.8 kpc (Masson 1989). This is higher by a factor of ~ 7 than the nebula's ionized mass. However, this object also contains additional mass in molecular form, having been detected in H_2 (Beckwith, Persson, & Gatley 1978) and CO (Bachiller et al. 1991). The 21 cm H I emission has been mapped in IC 418 (Taylor & Pottasch 1987; Taylor et al. 1989). The latter authors derive an H I mass of 0.35 $M_\odot$ for an assumed distance of 1 kpc, at least some of it located at large distances (nearly 1 pc) from the central star. As for BD +30°3639, this is about an order of magnitude larger than the mass of the ionized gas. No evidence has been found for molecules in IC 418 (Zuckerman & Gatley 1988; H. L. Dinerstein, unpublished work).

Estimates for the neutral masses can also be made from the far-infrared "atomic" cooling lines, primarily [O I] 63 μm and [C II] 157 μm. Preliminary estimates for five nebulae (including BD +30°3639, IC 418, and NGC 7027) yield masses of 0.1–0.3 $M_\odot$ (Dinerstein et al. 1991, 1995a, b). However, these estimates rely heavily on the strength of the [C II] line and involve the assumption that the line strength scales directly with the carbon abundance. They also sample only gas that is warm enough ($T \geq 100$–200 K) to emit these particular lines, and will not arise from any material that is substantially cooler. For these reasons, these inferred masses are probably lower limits.

It is also difficult to derive reliable estimates of the molecular mass, for various reasons. Although H_2 emission has been seen in a large number of nebulae, mere detection is insufficient for a mass determination. One needs to understand the line excitation mechanism, which is still somewhat controversial (see Dinerstein et al. 1988; Huggins 1993), as well as to measure accurate integrated fluxes for the entire line-emitting region. On the other hand, mass determinations from CO depend on correctly estimating the CO/H_2 ratio in these regions, where standard interstellar values are unlikely to apply because of partial photodissociation by the central star's radiation field; however, estimated values fall in the range 0.001–1 $M_\odot$ (Huggins & Healey 1989).

6.3. *The Origin of the* Na I *Features*

We concluded in § 6.1 that the Na I lines track the "atomic" indicators, H I and [O I], more closely than the molecular ones. That is, in order to produce detectable Na I features it is sufficient that a nebula have a circumnebular atomic zone; a molecular component is not necessary. This suggests strongly that at least some, if not most, of the Na I absorption is within the photodissociated region. In fact, because of radiative transfer effects, the addition of a molecular region apparently does not always increase the strength of the Na I absorptions. For example, IC 4997 has Na I absorption features that are nearly as strong (in central depth and equivalent width) as those of BD +30°3639, although so far there is no evidence for molecules in IC 4997. The Na I absorptions in NGC 6302 and Sw St 1, both of which contain molecules, have small absorption equivalent widths, but are obviously projected onto emission components.

We can ask whether it is plausible that detectable Na I features are formed within the dissociation regions. It is tempting to make an analogy with diffuse interstellar material, where Na I lines are observed in regions where only a tiny fraction of the gas-phase sodium is neutral. This fraction is usually estimated from a simple calculation balancing photoionization with recombination (e.g., Phillips et al. 1984). This implicitly one-zone treatment is obviously inadequate for planetary nebulae. More relevant for our purposes are models such as those of van Dishoeck & Black (1986), who calculate the internal chemical and ionization structure of interstellar clouds in ambient UV radiation fields. They present a variety of models for interstellar clouds with $0.8 < A_V < 1.5$, but with fairly low densities (mostly less than 500 cm^{-3}) and UV radiation fields only few times stronger than the "standard" interstellar value. A typical value for the column-averaged neutral sodium fraction f(Na I) = N(Na I)/N(Na) in these models is 0.05. However, their assumed UV radiation field is much weaker than in the case of the planetary nebula envelopes.

Most applicable are "PDR" models such as those of Tielens & Hollenbach (1985). Such models have not yet been calcu-

lated specifically for planetary nebulae, where the geometry is spherical rather than one-dimensional, and the composition is different from that of the "standard" ISM, being very carbon-rich. (Since it is the major coolant and electron donor in the PDR, changes in the carbon abundance potentially can have a major impact on the overall thermal and ionization structure of the PDR). However, based on the existing PDR models, calculated for an oxygen-rich composition, it seems likely that the sodium neutral fraction is about 10^{-3}, within an order of magnitude, in the region where carbon is singly-ionized and hydrogen is atomic (Tielens 1993; Natta & Hollenbach 1994). This is in reasonable agreement with our measurements of the ratio N(Na I)/N(H I). One would expect that in the more predominantly molecular layers the sodium will become increasingly neutral; however, it seems unlikely that much of it goes into molecular form (see van Dishoeck & Black 1986) or is depleted significantly into grains (Phillips et al. 1984). Thus, the portion of the observed Na I lines formed in the atomic versus the molecular regions will depend on the location of the outer mass boundary and the proportion of the total column density that comprises each of these (crudely defined) layers, and therefore will be different for each nebula.

6.4. *Significance of the Detection Rate*

In assessing the significance of our detections, the reader must bear in mind that this is not an unbiased sample. The velocity criterion is neutral, but the other selection criteria bias the sample in different ways. The selection of some objects because of previous evidence for neutral or molecular material obviously favors detection. However, as we pointed out in § 2, the selection on the basis of visually bright central stars should bias the results *against* nebulae with very massive neutral shells. Bearing these caveats in mind, we can summarize our statistics on Na I absorptions as nine detections, eight significant nondetections, and four indeterminate cases, roughly a 50% success rate. We see Na I emission features in six objects if we include BD +30°3639, out of 19 possible candidates (emission features would not have been seen detected in NGC 6572 or Hb 12), for an effective detection rate of about 30%. However, as mentioned above, the detectability of the emission features depends particularly strongly on the instrumental setup and other factors. Given the various selection effects, we can say only that the presence of detectable Na I features is clearly a common phenomenon. Furthermore, despite the difficulty in estimating the exact fraction of sodium in neutral form, the derived column densities do suggest that nebulae with observable Na I must contain a substantial amount of neutral, if not necessarily molecular, material.

Part of the value of the Na I features for studies of neutral material in planetary nebulae is that at least in some cases the detection threshold is lower than for the other atomic techniques; more generally, different factors mitigate against the detection of Na I, H I, and [O I], respectively. The main limiting factor in detecting the [O I] 63 μm line has been the sensitivity of the Kuiper Airborne Observatory, with its modest collecting aperture (1 m). Since the line strength scales approximately with the radio continuum brightness of the ionized gas (Dinerstein et al. 1985, 1995a), [O I] can be measured only in nebulae with radio continuum flux densities $\geq$100 mJy. (This situation will change in the future, when more sensitive facilities become available, e.g. ISO, the Infrared Space Observatory, and SOFIA, the Stratospheric Observatory for Infrared Astronomy.) Detection of the 21 cm H I line in absorption also depends on the radio continuum strength, since it must be detected in absorption against this continuum, and it may be harder to measure in very dense objects, where the free-free emission begins to go optically thick at 1.4 GHz. The H I technique also suffers from the same problem as Na I, in terms of the "masking" of nebular features by foreground interstellar absorptions.

Nebulae with observed Na D lines should also be detectable in other similarly strong resonance lines. The optical spectral region contains only a handful of such lines from species that are the dominant ionization states in predominantly neutral gas (e.g., Ca II, K I, Ca I), and most of these are weaker than the Na D lines. Most of the strong resonance lines of abundant species from H I regions fall in the "satellite ultraviolet." A number of these lines were seen in the *IUE* high-resolution spectra of BD 30°3639 by Pwa, Pottasch, & Mo (1986), although those authors did not take them as definitive evidence for a neutral shell. We have reobserved selected sections of the UV spectrum containing absorption lines from species such as C I, C II, and O I, using the Goddard High-Resolution Spectrograph on the *Hubble Space Telescope* (Dinerstein et al. 1995b). Such measurements will help to constrain such properties of the neutral envelope as overall ionization balance, electron density, and gas temperature.

7. SUMMARY

We have observed 21 planetary nebulae in the region of the Na I D lines at high spectral resolution (10 km s^{-1}), in order to search for evidence of features associated with a neutral envelope. We detect nebular Na I absorptions in nine objects, and nebular Na I emission features in five; thus, about half the sample shows some kind of feature that we identify as nebular based on radial velocity coincidences. The statistical significance of our detection rate is unclear, since the selection criteria may have influenced our success rate, and in a few cases interstellar absorption would mask the nebular features. Nevertheless, we have clearly shown that detectable nebular Na I is common. We interpret this as evidence that a substantial fraction of planetary nebulae possess circumnebular neutral envelopes.

The detected Na I absorption features lie blueward of the nebular systemic velocity. We find that the Na I expansion velocity, derived by taking the difference between the Na I absorption minimum and the systemic velocity, is comparable to the expansion velocity of the ionized gas. Taylor et al. (1990) reached the same conclusion from observations of H I at 21 cm in planetary nebulae. In a few cases there appear to be blue wings or weak, high-velocity features in the Na I profiles, which might represent acceleration zones within the nebular envelope, or might arise from fast-moving low ionization clumps similar to those reported by Balick et al. (1993, 1994) in several planetary nebulae. Higher spectral resolution and signal-to-noise spectra would be useful to better define these blueshifted features and to obtain more accurate overall line profiles.

From a doublet-ratio analysis, we estimate Na I line-of-sight column densities ranging from a few times 10^{11} cm^{-2}, essentially our detection limit, to greater than 10^{13} cm^{-2}. We compare these values with the corresponding H I column densities determined from the 21 cm line and find values for the ratio N(Na I)/N(H I) of 10^{-9} to 10^{-8}. This number is higher than for diffuse interstellar clouds, implying that the sodium in the circumnebular envelopes is more fully shielded from UV

radiation than in the diffuse clouds. Since Na I is seen in some planetary nebulae which have also been detected in H I or [O I] but not in molecular species, it appears that detectable Na I features can be produced by the dissociated layers in a neutral envelope, and do not require that a molecular zone is present.

Our results imply that the outer portions of many planetary nebulae are neutral. These nebulae therefore must be radiation-bounded rather than mass-bounded, and the total amount of recently expelled material is larger than the ionized mass. Knowledge of the amount and distribution of this neutral material is essential for understanding and modeling the mass-loss episode that terminates the asymptotic giant phase of stellar evolution and produces a planetary nebula. The Na I lines, although formed by a trace species, can act as pointers that signal the presence of neutral material. They also offer information about the velocity of the outer nebular envelope, which is relevant to understanding the dynamical evolution of planetary nebulae.

We appreciate the helpful assistance of the support staff at McDonald and Kitt Peak Observatories, which made it possible to obtain these observations. This research was supported by NSF grant AST 91-15101 (H. L. D.) and AST 91-15026 (C. S.).

REFERENCES

Acker, A., Gleizes, F., Chopinet, M., Marcout, J., Ochsenbein, F., & Roques, J. M. 1982, Catalogue of the Central Stars of true and possible Planetary Nebulae (Strasbourg: Obs. de Strasbourg)
Allen, C. W. 1973, Astrophysical Quantities (London: Athlone), 31
Aller, L. H., & Keyes, C. D. 1988, Proc. Natl. Acad. Sci., 85, 2417
Altschuler, D. R., Schneider, S. E., Giovanardi, C., & Silverglate, P. R. 1986, ApJ, 305, L85
Bachiller, R., Gómez-González, J., Bujarrabal, V., & Martín-Pintado, J. 1988, A&A, 196, L5
Bachiller, R., Huggins, P. J., Cox, P., & Forveille, T. 1991, A&A, 247, 525
Bachiller, R., Huggins, P. J., Martín-Pintado, J., & Cox, P. 1992, A&A, 256, 231
Balick, B., Perinotto, M., Maccioni, A., Terzian, Y., & Hajian, A. 1994, ApJ, 424, 800
Balick, B., Rugers, M., Terzian, Y., & Chengalur, J. N. 1993, ApJ, 411, 778
Beckwith, S., & Natta, A. 1987, A&A, 181, 57
Beckwith, S., Persson, S. E., & Gatley, I. 1978, ApJ, 219, L33
Bianchi, L., & Falcetta, C. 1988, in Mass Outflows from Stars and Galactic Nuclei, ed. L. Bianchi & R. Gilmozzi (Dordrecht: Kluwer), 273
Deutsch, A. J. 1956, ApJ, 123, 210
———. 1960, in Stars and Stellar Systems, Vol. 6, Stellar Atmospheres, ed. J. L. Greenstein (Chicago: Univ. Chicago Press), 543
Dinerstein, H. L. 1991, PASP, 103, 861
———. 1995, in Asymmetrical Planetary Nebulae, ed. N. Soker & A. Harpaz (New York: AIP), in press
Dinerstein, H. L., Ellis, H. B., Haas, M. R., & Werner, M. W. 1985, BAAS, 17, 908
Dinerstein, H. L., Haas, M. R., Erickson, E. F., & Werner, M. W. 1995a, in The Galactic Ecosystem: From Gas to Stars to Dust, ed. M. R. Haas, J. A. Davidson, & E. F. Erickson (ASP Conf. Ser.), in press
Dinerstein, H. L., Haas, M. R., & Werner, M. W. 1991, BAAS, 23, 915
Dinerstein, H. L., Haas, M. R., Erickson, E. F., & Werner, M. W. 1995c, in preparation
Dinerstein, H. L., Lester, D. F., Carr, J. S., & Harvey, P. M. 1988, ApJ, 327, L27
Dinerstein, H. L., & Sneden, C. 1988, ApJ, 335, L23 (DS)
Dinerstein, H. L., Sneden, C., McQuitty, R., Danly, L., & Heap, S. 1995b, BAAS, 26, 1386
Ellis, H. B., & Werner, M. W. 1984, BAAS, 16, 463
Ferlet, R., Vidal-Madjar, A., & Gry, C. 1985, ApJ, 298, 838
Fitzpatrick, M. J., & Sneden, C. 1987, BAAS, 19, 1129
Gathier, R., Pottasch, S. R., & Goss, W. M. 1986, A&A, 157, 191
Gieseking, F., Becker, I., & Solf, J. 1985, ApJ, 295, L17
Heap, S. R., & Hintzen, P. 1990, ApJ, 353, 200
Huggins, P. J. 1992, in Mass Loss from Red Giants, ed. M. Morris & B. Zuckerman (Dordrecht: Reidel), 309
———. 1993, in IAU Symp. 155, Planetary Nebulae, ed. R. Weinberger & A. Acker (Dordrecht: Kluwer), 147
Huggins, P. J., & Healy, A. P. 1989, ApJ, 346, 201
Jacoby, G. H. 1988, ApJ, 333, 193
Jenkins, E. B. 1986, ApJ, 304, 739
Knapp, G. R. 1985, in Mass Loss from Red Giants, ed. M. Morris & B. Zuckerman (Dordrecht: Reidel), 171
Lenzuni, P., Natta, A., & Panagia, N. 1989, ApJ, 345, 306
Masson, C. R. 1989, ApJ, 346, 243
Meaburn, J., & Walsh, J. R. 1980, MNRAS, 193, 631
Melnick, G., Russell, R. W., Gull, G. E., & Harwitt, M. 1981, ApJ, 243, L35
Mendéz, R. H., Kudritzki, R. P., Herrero, A., Husfeld, D., & Groth, H. G. 1988, A&A, 190, 113
Miranda, L. F., & Solf, J. 1991, A&A, 252, 331
Morton, D. C., & Smith, W. H. 1973, ApJS, 26, 333
Mufson, S. L., Lyon, J., & Marionni, P. A. 1975, ApJ, 201, L85
Münch, G. 1968, in Stars and Stellar Systems, Vol. 7, Nebulae and Interstellar Matter, ed. B. M. Middlehurst & L. H. Aller (Chicago: Univ. Chicago Press), 365
Nachman, P., & Hobbs, L. M. 1973, ApJ, 182, 481
Natta, A., & Beckwith, S. 1986, A&A, 158, 310
Natta, A., & Hollenbach, D. J. 1994, private communication
O'Dell, C. R., & Ball, M. E. 1985, ApJ, 289, 526
Payne, H. E., Phillips, J. A., & Terzian, Y. 1988, ApJ, 326, 368
Peimbert, M., & Torres-Peimbert, S. 1983, in IAU Symp. 103, Planetary Nebulae, ed. D. R. Flower (Dordrecht: Reidel), 233
Perek, L., & Kohoutek, L. 1967, Catalogue of Galactic Planetary Nebulae (Prague: Czechoslovak Acad. Sci.)
Phillips, A. P., Pettini, M., & Gondhalekar, P. M. 1984, MNRAS, 206, 337
Pottasch, S. R. 1980, A&A, 89, 336
———. 1988, in Mass Outflows from Stars and Galactic Nuclei, ed. L. Bianchi & R. Gilmozzi (Dordrecht: Kluwer), 109
Pottasch, S. R., Goss, W. M., Arnal, E. M., & Gathier, R. 1982, A&A, 106, 229
Pwa, T. H., Pottasch, S. R., & Mo, J. E. 1986, A&A, 164, 184
Rodríguez, L. F. 1989, in IAU Symp. 131, Planetary Nebulae, ed. S. Torres-Peimbert (Dordrecht: Kluwer), 129
Rodríguez, L. F., & Moran, J. M. 1982, Nature, 299, 323
Rodríguez, L. F., García-Barreto, J. A., & Gómez, Y. 1985, RevMexAA, 11, 109
Sabbadin, F. 1984, A&AS, 58, 273
Schneider, S. E., Silverglate, P. R., Altschuler, D. R., & Giovanardi, C. 1987, ApJ, 314, 572
Schneider, S. E., Terzian, Y., Purgathofer, A., & Perinotto, M. 1983, ApJS, 52, 399
Seaquist, E. R., & Davis, L. E. 1983, ApJ, 274, 659
Shaw, R. A., & Kaler, J. B. 1985, ApJ, 295, 537
———. 1989, ApJS, 69, 495
Spergel, D. N., Giuliani, J. L., & Knapp, G. R. 1983, ApJ, 275, 330
Spitzer, L., Jr. 1968, Diffuse Matter in Space (New York: Wiley)
Strömgren, B. 1948, ApJ, 108, 242
Taylor, A. R., Gussie, G. T., & Goss, W. M. 1989, ApJ, 340, 932
Taylor, A. R., Gussie, G. T., & Pottasch, S. R. 1990, ApJ, 351, 515
Taylor, A. R., & Pottasch, S. R. 1987, A&A, 176, L5
Tielens, A. G. G. M. 1993, in IAU Symp. 155, Planetary Nebulae, ed. R. Weinberger & A. Acker (Dordrecht: Kluwer), 155
Tielens, A. G. G. M., & Hollenbach, D. J. 1985, ApJ, 291, 722
Treffers, R. T., Fink, U. F., Larson, P. L., & Gautier, N. T. 1976, ApJ, 209, 793
van Dishoeck, E. F., & Black, J. H. 1986, ApJS, 62, 109
Weinberger, R. 1989a, A&AS, 78, 301
———. 1989b, in IAU Symp. 131, Planetary Nebulae, ed. S. Torres-Peimbert (Dordrecht: Kluwer), 93
Welsh, B. Y., Vedder, P. W., & Vallerga, J. V. 1990, ApJ, 358, 473
Willmarth, D. 1987, A CCD Atlas of Comparison Spectra: Thorium-Argon Hollow Cathode 3180 Å–9540 Å (Tucson: NOAO)
———. 1988, Instrumentation Operation Manual: Echelle Spectrograph (Tucson: NOAO)
Zuckerman, B., & Gatley, I. 1988, ApJ, 324, 501